

# Island-size distribution and capture numbers in three-dimensional nucleation: Dependence on island morphology

John Royston\* and Jacques G. Amar†

*Department of Physics & Astronomy, University of Toledo, Toledo, Ohio 43606, USA*

(Received 17 February 2009; revised manuscript received 5 August 2009; published 13 October 2009; publisher error corrected 25 June 2010)

The scaling of the monomer and island densities, island-size distribution (ISD), and capture-number distribution (CND) as a function of the fraction of occupied sites (coverage) and ratio  $D_h/F$  of the monomer hopping rate  $D_h$  to the (per site) monomer creation rate  $F$  are studied for the case of irreversible nucleation and growth of fractal islands in three dimensions ( $d=3$ ). We note that our model is a three-dimensional analog of submonolayer growth in the absence of island relaxation and may also be viewed as a simplified model of the early stages of vacancy cluster nucleation and growth under irradiation. In contrast to results previously obtained for point-islands in  $d=3$ , for which mean-field behavior corresponding to a CND which is independent of island size was observed, our results indicate that for fractal islands the scaled CND increases approximately linearly with island size in the asymptotic limit of large  $D_h/F$ . In addition, while the peak height of the scaled ISD for fractal islands appears to diverge with increasing  $D_h/F$ , the dependence on  $D_h/F$  is much weaker than for point-islands in  $d=3$ . The results of a self-consistent rate-equation calculation for the coverage and  $D_h/F$  dependence of the average island and monomer densities are also presented and good agreement with simulation results is obtained. For the case of point-islands, the value of the exponent  $\chi$  describing the  $D_h/F$  dependence of the island density at fixed coverage, e.g.,  $N_{sat} \sim (D_h/F)^{-\chi}$ , is in good agreement with the value ( $\chi=1/3$ ) expected for irreversible growth. However, for both compact and fractal islands in  $d=3$ , our results indicate that the value of  $\chi$  ( $\chi \approx 0.42$ ) is significantly larger. In order to explain this behavior, an analytical expression [e.g.,  $\chi = d_f / (3d_f - 2)$ ] for the dependence of  $\chi$  on island fractal dimension  $d_f$  in  $d=3$  is derived and found to give reasonable agreement with our simulation and rate-equation results for the case of point-islands ( $d_f = \infty$ ), compact islands ( $d_f = 3$ ), and fractal islands ( $d_f \approx 2.5$ ). A general expression for the exponent  $\chi$ , valid for  $d \geq 2$ , as a function of the critical island size  $i$  and  $d_f$  is also derived.

DOI: [10.1103/PhysRevE.80.041602](https://doi.org/10.1103/PhysRevE.80.041602)

PACS number(s): 81.15.Aa, 68.55.A-, 68.43.Hn

## I. INTRODUCTION

The ordering and size distribution of islands in the submonolayer growth regime plays an important role in determining the later stages of thin-film growth [1–5]. Accordingly, considerable theoretical effort has been carried out toward an understanding of the island-size distribution  $N_s(\theta)$  (where  $N_s$  is the number density of islands of size  $s$  at coverage  $\theta$ ) and its dependence on growth conditions [3,4,6–24]. In particular, it is known that in the precoalescence regime the island-size distribution (ISD) satisfies the scaling form [8,9],

$$N_s(\theta) = \frac{\theta}{S^2} f\left(\frac{s}{S}\right), \quad (1)$$

where  $S$  is the average island size, and the scaling function  $f(u)$  depends on the critical island size and island morphology [12].

One approach to nucleation and growth is the use of rate equations (REs) [4,6,25]. For the case of irreversible growth, REs valid in the precoalescence regime may be written in the form,

$$\frac{dN_1}{d\theta} = 1 - 2R\sigma_1 N_1^2 - RN_1 \sum_{s=2}^{\infty} \sigma_s N_s - \kappa_1 N_1 - \sum_{s=1}^{\infty} \kappa_s N_s, \quad (2)$$

$$\frac{dN_s}{d\theta} = R\sigma_{s-1} N_1 N_{s-1} - R\sigma_s N_1 N_s + \kappa_{s-1} N_{s-1} - \kappa_s N_s \quad (s \geq 2), \quad (3)$$

where  $R=D/F$  is the ratio of the monomer diffusion rate  $D$  to the (per site) deposition rate  $F$ , the capture numbers  $\sigma_s$  ( $\sigma_1$ ) correspond to the average capture rate of diffusing monomers by islands of size  $s$  (monomers), and the terms with  $\kappa_s$  correspond to direct impingement. In this approach, the central problem is the determination of the size- and coverage-dependent capture numbers  $\sigma_s(\theta)$ .

The simplest possible assumption for the capture-number distribution (CND) is the mean-field (MF) assumption  $\sigma_s(\theta) = \sigma_{av}(\theta)$ . However, using kinetic Monte Carlo (KMC) simulations, Bartelt and Evans [13] showed that in  $d=2$  [corresponding to a two-dimensional (2D) substrate], due to the existence of a strong correlation between the size  $s$  of an island and the size of the surrounding capture zone, there is a nontrivial dependence of the capture number on the island size even for the case of point-islands. They also showed that in the asymptotic limit of large  $D/F$ , the scaled ISD is related to the scaled CND as

\*jroysto@utnet.utoledo.edu  
†jamar@physics.utoledo.edu

$$f(u) = f(0) \exp \left[ \int_0^u dx \frac{2z - 1 - C'(x)}{C(x) - zx} \right], \quad (4)$$

where  $C(s/S) = \sigma_s / \sigma_{av}$  is the scaled CND,  $z$  is the dynamical exponent describing the dependence of the average island size on coverage ( $S \sim \theta^z$ ), and  $f(0)$  is determined by the normalization condition  $\int_0^\infty du f(u) = 1$ . Using Eq. (4), one can show that for  $z < 1$  the mean-field assumption  $\sigma_s(\theta) = \sigma_{av}$  or  $C(u) = 1$  implies that in the asymptotic limit of large  $D/F$ , the scaled ISD may be written as

$$f(u) = (1 - z)(1 - zu)^{1/z-2}. \quad (5)$$

We note that for point-islands, one has  $z = 2/3$  and therefore the MF approximation implies that in the asymptotic limit one has  $f(u) = \frac{1}{3}(1 - 2u/3)^{-1/2}$ , which leads to a divergence in the scaled ISD at  $u = 3/2$ .

Recently Shi, Shim, and Amar (SSA) [26,27] carried out KMC simulations of point-island models of irreversible growth in  $d=3$  and  $d=4$  in order to understand the effects of substrate dimension  $d$  on the scaled ISD and CND. In contrast to the nontrivial behavior obtained [13] for point-islands in  $d=2$ , the mean-field behavior was observed in  $d=3$  and  $d=4$ . In particular, the capture number was found to be independent of island size for large  $D/F$ , while the ISD diverged with increasing  $D/F$ . These results clearly demonstrated that for point-islands, the substrate dimension has a significant effect on the scaled ISD and CND. We note that in three dimensions (3D), this model may also be considered to be a simplified model of vacancy formation and vacancy cluster nucleation during irradiation.

Here we consider the irreversible nucleation and growth of *fractal* islands in  $d=3$ . We note that this is a more realistic model than the point-island model (since it corresponds to irreversible nucleation and growth in the absence of relaxation) and is also of particular interest since we would like to determine the dependence of the scaling behavior on the island fractal dimension  $d_f$ . In contrast to results previously obtained for point-islands in  $d=3$ , for which mean-field-like behavior corresponding to a CND which is independent of island size was observed, our results indicate that for fractal islands in  $d=3$  the scaled CND increases approximately linearly with island size. In addition, we find that while the scaled ISD for fractal islands appears to diverge with increasing  $D_h/F$ , it diverges much more slowly than for point-islands in  $d=3$ . For comparison, we also present results for the case of fractal islands in  $d=2$ .

In order to understand the scaling behavior of the average island and monomer densities for extended islands in  $d=3$ , the results of a self-consistent RE calculation are also presented and compared with the corresponding simulation results. Somewhat surprisingly, our results indicate that for both fractal and compact islands (with  $d_f \approx 2.5$  and 3, respectively), the value of the exponent  $\chi$  describing the  $D/F$  dependence of the island density at fixed coverage is significantly larger in  $d=3$  than the value ( $\chi \approx 1/3$ ) [6] expected for irreversible growth (and typically observed in  $d=2$  and for point-islands in  $d=3$ ). In order to explain this behavior, a general analytical expression for the dependence of  $\chi$  on

island fractal dimension  $d_f$  in  $d=3$  is derived and found to give reasonable agreement with our KMC results.

This paper is organized as follows. In Sec. II, we first describe the details of our simulations. In Sec. III A, we present our KMC results for the average monomer and island densities, along with analytical results for the exponent  $\chi$  describing the dependence of the island density  $N$  on  $D/F$ . For completeness, we also present the results of a self-consistent RE calculation, which leads to good agreement with KMC simulations for the coverage dependence of the average monomer density  $N_1(\theta)$  and average island density  $N(\theta)$ . We then present our KMC results for the scaled island-size and capture-number distributions in Sec. III B. Finally, in Sec. IV, we discuss our results.

## II. MODEL AND SIMULATIONS

While most of the results presented here are for the irreversible growth of fractal islands in  $d=3$ , for comparison we have also carried out simulations of the corresponding point-island model. In both the point-island and fractal models, monomers are randomly created at empty sites on a cubic lattice, with creation rate  $F$  per site per unit time, and then hop randomly in each of the 6 nearest-neighbor directions with hopping rate  $D_h$ . As in previous studies of irreversible nucleation and growth [9], we assume that dimers are stable and do not break up and that any particle with one or more occupied nearest-neighbor sites is “frozen.” Thus, the key parameter in our model is the ratio  $R_h = D_h/F$  of the monomer hopping rate to the deposition rate. Alternatively, one may consider the ratio  $R = D/F = R_h/6$ , where  $Da^2$  is the monomer diffusion constant and  $a$  is the lattice constant.

Since for extended islands two particles cannot occupy the same site, for the fractal model we have used two methods to avoid deposition of a particle on a previously occupied site. In the first method, if an already-occupied site is selected for deposition, the deposition is rejected and another site is randomly selected. In the second method, the nearest-unoccupied site was selected. In general, we found a negligible difference between the two methods. We note that the point-island model studied here is also somewhat different from that previously studied by Shim *et al.* in Ref. [26] (SSA model), although it is similar to the 2D point-island models previously studied by Bartelt and Evans in Ref. [13]. In particular, if any particle is deposited at or moves to an unoccupied site, which has an occupied nearest neighbor, then that particle is “absorbed” by the occupied site and the island size increases by 1. Similarly, if a particle is deposited on an occupied site then it is also absorbed by that site. In contrast, for the previously studied SSA model [26], it was necessary for a particle to land on an already-occupied site before that particle would be absorbed. Thus, the point-island model studied here has a range of interaction, which is equivalent to that of the fractal model, and which is slightly larger [28] than that for the SSA model.

In order to study the asymptotic scaling behavior, we have carried out simulations for values of  $R_h$  ranging from  $10^6$  to  $10^{10}$ . To avoid finite-size effects, simulations were carried out using a system size  $L=200$ , while averages were taken

over 200 runs. For each set of parameters, the scaled ISD and CND as well as the average island density  $N(\theta)$  and monomer density  $N_1(\theta)$  were obtained for coverages up to  $\theta=0.1$ , which is somewhat beyond the onset of coalescence for large  $D_h/F$ .

In order to calculate the CND, we have followed the method outlined in Ref. [13]. In particular, the CND  $\sigma_s(\theta)$  was calculated by using the equation  $\sigma_s(\theta) = n_s^c / (R\Delta\theta N_1 N_s L^3)$ , where  $n_s^c$  is the number of monomer capture events corresponding to an island of size  $s$  during a small coverage interval ( $\Delta\theta \approx 0.05\theta$ ). As in Ref. [13], the island size  $s$  at the beginning of the coverage interval was used when incrementing the counter  $n_s^c$  in order to obtain good statistics.

### III. RESULTS

#### A. Island and monomer densities

##### 1. Self-consistent rate-equation approach

Before presenting our simulation results, we first consider a self-consistent rate-equation approach to calculating the island-size distribution  $N_s(\theta)$  and capture number  $\sigma_a(\theta)$  following the method originally developed by Bales and Chrzan [11]. While such an approach is not expected to give accurate results for the ISD and CND since correlations are not taken into account, in previous work [11,26,27] it has been shown to give accurate quantitative results for the average island and monomer densities  $N(\theta) = \sum_{s \geq 2} N_s(\theta)$  and  $N_1(\theta)$ . As in Ref. [26], we consider a quasistatic diffusion equation for the monomer density  $n_1(\vec{r})$  surrounding an island of size  $s$  of the form,

$$\nabla^2 n_1(\vec{r}) - \xi^{-2}(n_1 - N_1) = 0, \quad (6)$$

where  $N_1$  is the average monomer density and  $\xi$  corresponds to an overall average capture term. For consistency with the REs (2) and (3), we require

$$\xi^{-2} = 2\sigma_1 N_1 + \sum_{s=2}^{\infty} \sigma_s N_s. \quad (7)$$

Assuming spherical symmetry and solving for  $n_1(r)$  using the boundary conditions  $n_1(\infty) = N_1$  and  $n_1(r_s) = 0$ , where  $r_s = r_0 s^{1/d_f}$  is the radius of an island of size  $s$  and  $d_f$  is the island fractal dimension, the following expression for  $n_1(r)$  may be obtained [26]:

$$n_1(r) = N_1 [1 - (r_s/r) e^{-(r-r_s)/\xi}]. \quad (8)$$

This leads to the following expression for the capture number [26]:

$$\sigma_s = \frac{4\pi r_s^2}{N_1} \left( \frac{\partial n_1}{\partial r} \right)_{r=r_s} = 4\pi r_s (1 + r_s/\xi). \quad (9)$$

We note that for a given distribution  $N_s(\theta)$ , the capture length  $\xi$  may be determined self-consistently using Eqs. (7) and (9).

##### 2. Comparison with KMC results

Using Eq. (9), we have numerically integrated the rate equations (2) and (3) for both the fractal and point-island

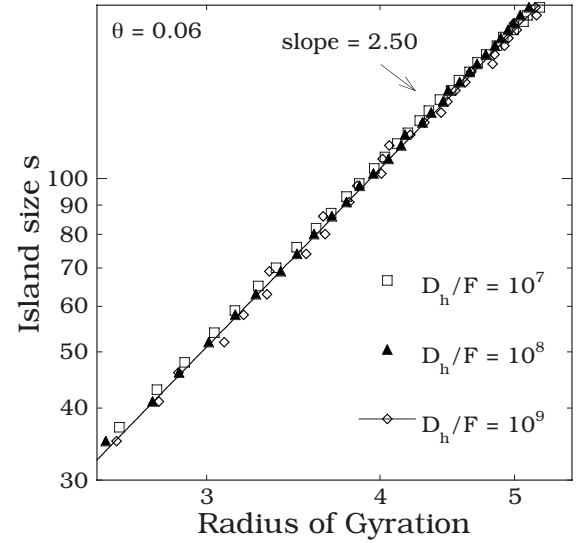


FIG. 1. Island size  $s$  vs radius of gyration  $R_G$  for fractal islands with  $R_h = 10^7 - 10^9$  and coverage  $\theta = 0.06$ .

models in  $d=3$  and compared with our KMC simulations. We note that  $r_0$  is a fitting parameter, which may be different for fractal and point-islands. However, we find that approximately the same value of  $r_0$  (e.g.,  $r_0 \approx 1.0$ ) gives good agreement with our simulations for both point and fractal islands. This is perhaps not surprising because the range of interaction is the same in both of these models. We also note that this value is comparable to that used in previous simulations of fractal islands in 2D ( $r_0 = 1.0$ ) by Bales and Chrzan [11]. However, it is significantly larger than the value ( $r_0 \approx 1/3$ ) used in previous RE calculations for the SSA point-island model [26] in  $d=3$ , for which the range of interaction is significantly shorter.

In our RE calculations, we assumed  $d_f = \infty$  for point-islands and  $d_f \approx 2.5$  for the fractal-island model. The latter value is in good agreement with the measured value obtained in our fractal-island KMC simulations, as can be seen from Fig. 1, which shows the dependence of the average radius of gyration  $r_G = [\frac{1}{s} \sum_{i=1}^s (\mathbf{r}_i - \bar{\mathbf{r}})^2]^{1/2}$  (where  $\bar{\mathbf{r}} = \sum \mathbf{r}_i / s$ ) on island size  $s$ . This value is also in good agreement with well-known results for diffusion-limited aggregation [29] in 3D [30]. As already noted in Sec. II, for the fractal model we have carried out KMC simulations both with and without direct impingement, and a negligible difference was found between the two methods. However, for comparison we have also carried out RE calculations for both cases. In particular, in the case without impingement, we have assumed  $\kappa_s = 0$ , while in the case of direct impingement (with the deposited particle moved to the nearest-unoccupied site) we have assumed  $\kappa_s = s^{d/d_f}$  with  $d=3$ . We note that this expression for  $\kappa_s$  is the same as was assumed in Ref. [11] for the case of fractal islands in  $d=2$ . We also note that for compact (point) islands with  $d_f = d$  ( $d_f = \infty$ ), this expression implies  $\kappa_s = s$  ( $\kappa_s = 1$ ) as expected.

Figure 2 shows a comparison between our RE and KMC results for the island density  $N$  and monomer density  $N_1$  as a function of coverage for both the fractal and point-island models for values of  $D_h/F$  ranging from  $10^7$  to  $10^9$ . Since for the case of fractal islands, there was negligible difference

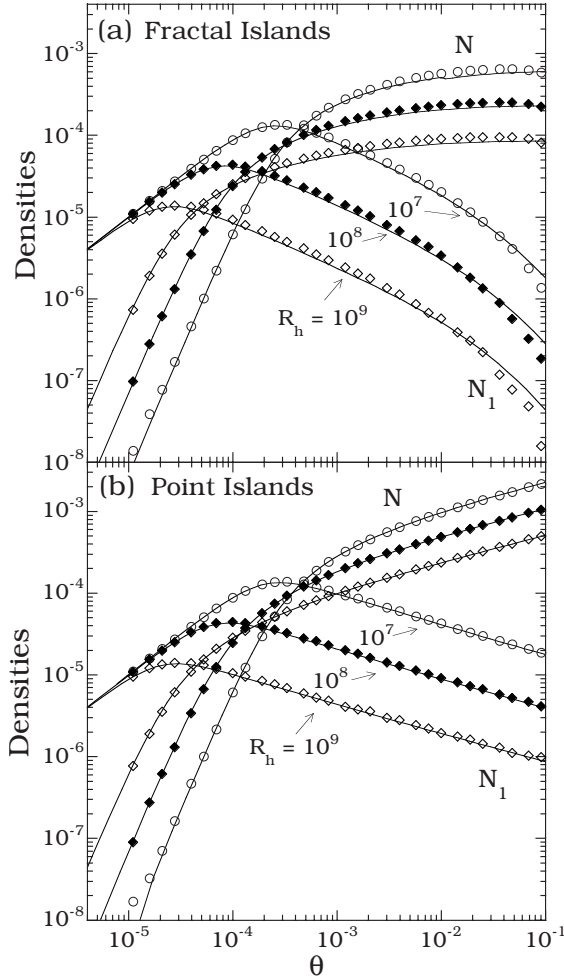


FIG. 2. Comparison between KMC results (symbols) and RE results (solid lines) for monomer density  $N_1(\theta)$  and island density  $N(\theta)$  as a function of coverage for  $R_h=10^7-10^9$  for (a) fractal islands and (b) point-islands.

between the KMC results with and without direct impingement, while the differences between our RE results with and without direct impingement were also relatively small, here we show only the KMC and RE results without impingement. As can be seen, there is good agreement between our KMC simulation results and the corresponding RE results. In addition, while the island density increases as  $N \sim \theta^{1-z} \sim \theta^{1/3}$  for large coverage in the point-island model, for the fractal model the island density saturates, thus, indicating that  $z=1$ , as expected for extended islands [9,10]. However, for  $\theta > 0.06$ , the island density decreases somewhat due to the onset of coalescence.

### 3. Dependence of $\chi$ on fractal dimension $d_f$

We now consider the dependence of the island density  $N$  at fixed coverage  $\theta$  on  $D/F$ . According to classical nucleation theory [6], for the case of irreversible growth with a critical island size of 1 (where the critical island size  $i$  corresponds to one less than the size of the smallest stable island), one expects  $N \sim (D/F)^{-\chi}$ , where  $\chi=1/3$ . As can be seen in Fig. 3, the measured value of  $\chi$  for the point-island

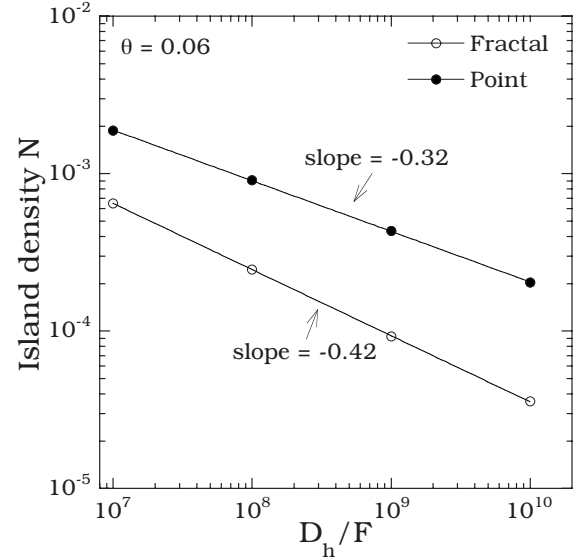


FIG. 3. Island density at coverage  $\theta=0.06$  as function of  $D_h/F$  for both fractal and point-island models.

model is in good agreement with this prediction. However, for the fractal model a significantly larger value, e.g.,  $\chi \approx 0.42$  is obtained. This large value of  $\chi$  can be explained as follows.

We first note that in the asymptotic limit of large  $D/F$ , the self-consistency condition Eq. (7) can be approximately written as

$$\frac{1}{\xi^2} = N\sigma_{av} = \theta\sigma_{av}/S, \quad (10)$$

where  $\sigma_{av} = \frac{1}{N} \sum_{s \geq 2} \sigma_s N_s$ . Using Eq. (10), along with the capture-number expression Eq. (9) and assuming that  $\sigma_{av} \sim \sigma_s$ , where  $S$  is the average island size, one obtains,

$$r_s/\xi \sim [\theta S^{(3-d_f)/d_f}]^{1/2} \quad (r_s/\xi \leq 1), \quad (11a)$$

$$r_s/\xi \sim \theta S^{(3-d_f)/d_f} \quad (r_s/\xi \geq 1). \quad (11b)$$

We note that Eq. (11) implies the existence of a critical coverage  $\theta_c \sim S^{-(3-d_f)/d_f}$  such that  $r_s/\xi < 1$  for  $\theta < \theta_c$  and  $r_s/\xi \geq 1$  for  $\theta \geq \theta_c$ . We also note that for point-islands with  $d_f = \infty$  (for which the island density never saturates, e.g., nucleation never ceases),  $\theta_c$  diverges with increasing  $D/F$  which implies  $r_s/\xi < 1$  for all finite values of  $\theta$ . Assuming  $S \approx \theta/N$  and  $N \sim R^{-\chi}$ , we obtain [ignoring the  $\theta$  dependence of  $\sigma(R, \theta)$ ],

$$\sigma_{av} \sim R^{\chi/d_f} \quad (r_s/\xi \leq 1), \quad (12a)$$

$$\sigma_{av} \sim R^{\chi(4/d_f-1)} \quad (r_s/\xi \geq 1). \quad (12b)$$

As Eq. (11) indicates, for compact and especially for fractal islands, it is possible that for large enough coverage one has  $r_s/\xi \geq 1$ , and, as a result, the second term in Eq. (9) dominates. However, in this case since the average island radius is significantly larger than the capture length  $\xi$  (which can be no larger than the typical distance between island perimeters), one expects that almost all monomers will attach to

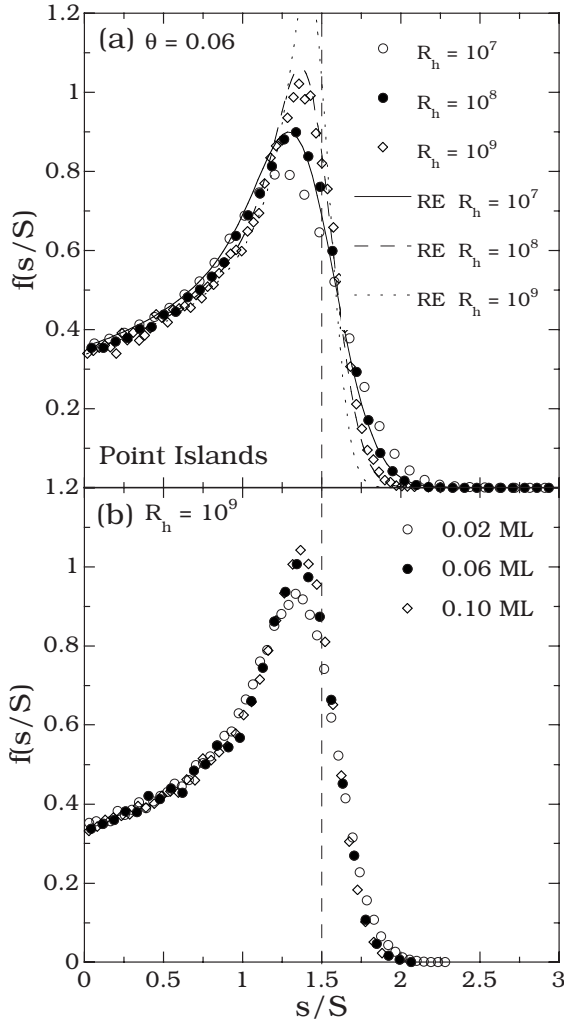


FIG. 4. Simulation results for scaled ISD for point-islands as a function of (a)  $R_h$  at fixed coverage  $\theta=0.06$  and (b) coverage for fixed  $R_h=10^9$ . Solid and dashed curves indicate corresponding RE results.

existing islands and nucleation will be minimal. Accordingly we expect Eq. (12a) holds in general for all coverages in the precoalescence regime for which there is still significant nucleation (e.g.,  $r_s/\xi \leq 1$ ).

The exponent  $\chi$  may now be obtained by considering the truncated rate equation,

$$\frac{dN_1}{d\theta} \approx 1 - R\sigma_{av} N_1 N. \quad (13)$$

In the limit of large  $D/F$  and beyond the nucleation regime, we have in the steady state  $dN_1/d\theta \approx 0$ , which implies

$$N_1 \sim (R\sigma_{av} N)^{-1}. \quad (14)$$

Substituting Eq. (14) into the truncated RE,

$$\frac{dN}{d\theta} = R\sigma_1 N_1^2, \quad (15)$$

we find

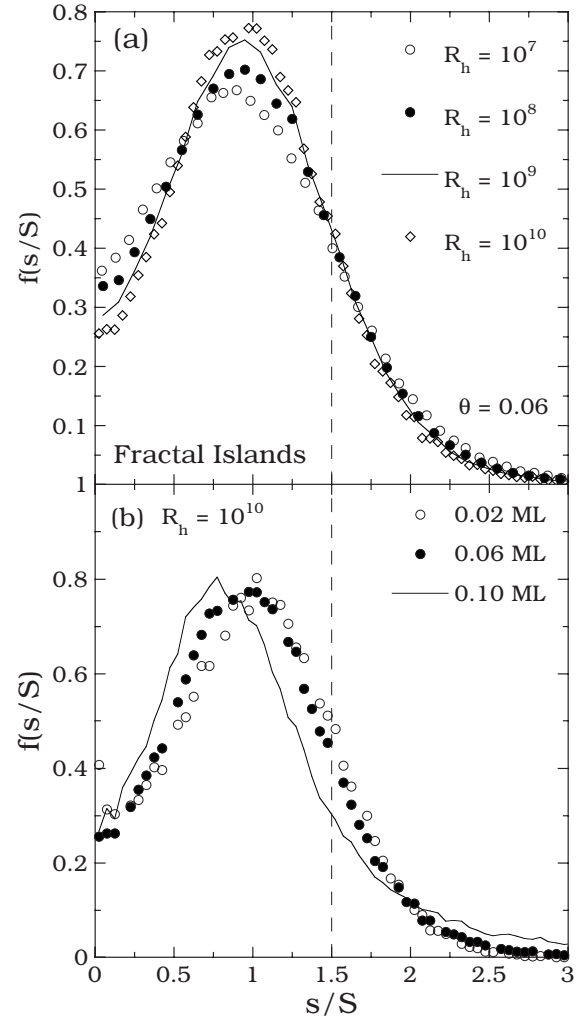


FIG. 5. Scaled ISD for fractal islands as a function of (a)  $R_h$  at fixed coverage  $\theta=0.06$  and (b) coverage for fixed  $R_h=10^{10}$ .

$$\frac{dN}{d\theta} \sim \frac{1}{\sigma_{av}^2(R, \theta) R N^2}. \quad (16)$$

Substituting Eq. (12a) into Eq. (16) and integrating [ignoring the dependence of  $\sigma_{av}(R, \theta)$  on  $\theta$ ] yields,

$$\chi = \frac{d_f}{3d_f - 2}. \quad (17)$$

For point-islands with  $d_f = \infty$ , this implies  $\chi = 1/3$  in good agreement with the results shown in Fig. 3 as well as with the standard prediction [6] for irreversible growth. In addition, for fractal islands with  $d_f = 2.5$ , Eq. (17) implies  $\chi \approx 0.45$ , which is in reasonable agreement with the value obtained in our simulations ( $\chi \approx 0.42$ ). Finally, we note that for compact islands with  $d_f = 3$ , Eq. (17) implies that  $\chi = 3/7 \approx 0.43$ . While we have not carried out KMC simulations for this case, this is in good agreement with self-consistent RE results we have obtained (not shown) for  $d_f = 3$ .

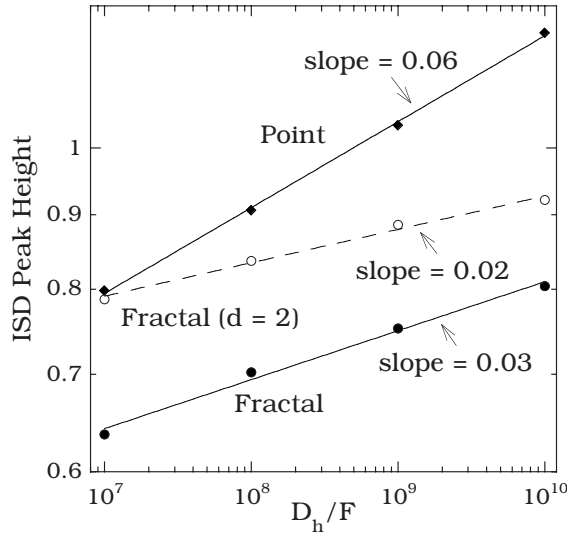


FIG. 6. Log-log plot of peak height of scaled ISD as function of  $D_h/F$  for fractal- and point-island models.

### B. Island-size and capture-number distributions

We now present our simulation results for the dependence of the scaled ISD and CND on  $D/F$ . We first consider the point-island model. As can be seen in Fig. 4(a), in this case the peak of the scaled ISD increases with increasing  $D/F$  indicating a divergence in the asymptotic limit of large  $D/F$ . This behavior is in good agreement with that previously obtained in Ref. [26] for a slightly different point-island model in  $d=3$ . We also note that the peak of the scaled ISD occurs for  $s/S > 1$  and appears to be shifting to the right with increasing  $D/F$ . There is also good scaling as a function of coverage as indicated by Fig. 4(b). Also shown in Fig. 4(a) are the corresponding RE results (solid and dashed curves). As can be seen, the RE prediction diverges somewhat faster than the simulation results.

We now consider the case of fractal islands. As can be seen in Fig. 5(a), the peak of the scaled ISD increases much less rapidly with increasing  $D/F$  than for the point-island model, while the shift of the peak position with increasing  $D/F$  is also significantly reduced. Since they disagree with simulations (the scaled ISD is significantly more sharply peaked and shifted to the right), the corresponding self-consistent RE results are not shown. We also note that as shown in Fig. 5(b), the scaled ISD exhibits relatively little dependence on coverage in the pre-coalescence regime ( $\theta \leq 0.06$ ). However at  $\theta=0.1$ , coalescence leads to a significant shift of the ISD peak as well as an extended tail for large  $s/S$ .

The dependence of the ISD peak height on  $D/F$  is shown in Fig. 6 for both point and fractal islands. As can be seen, for the case of point-islands, the ISD peak height increases with  $D/F$  as  $f_{pk}(D/F) \sim (D/F)^\phi$ , where  $\phi \approx 0.06$  in good agreement with previous results obtained in Ref. [26] using a slightly different point-island model. However, for the fractal model the exponent  $\phi$  ( $\phi \approx 0.03$ ) is significantly smaller. We note that a semilog plot gives an equally good fit, thus, indicating a possible logarithmic divergence. For comparison,

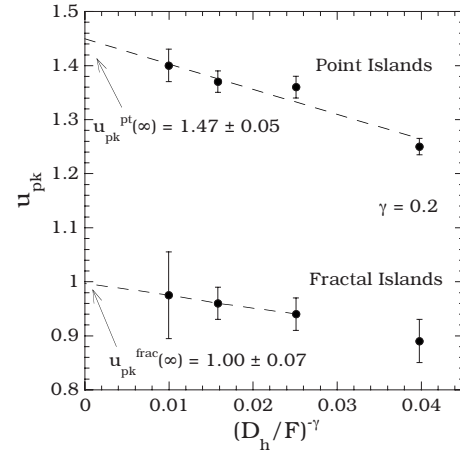


FIG. 7. Peak position  $u_{pk}$  of scaled ISD as a function of  $R_h^{-\gamma}$  for fractal- and point-island models with  $R_h=10^7-10^{10}$  and  $\theta=0.06$ . The value of  $\gamma=0.20$  was chosen for the best fit to the data.

also shown in Fig. 6 is the ISD peak height for fractal islands in  $d=2$ . As can be seen, in this case the value of  $\phi$  is even lower ( $\phi \approx 0.02$ ).

In order to determine the asymptotic peak position of the scaled ISD, we have considered a fit of the form  $u_{pk}(D/F) = u_{pk}(\infty) - A(D/F)^{-\gamma}$  and have varied the value of  $\gamma$  to obtain the best fit. In agreement with previous results for the point-island model studied in Ref. [26], we find that  $\gamma \approx 0.2$  gives the best fit. As shown in Fig. 7, we find a reasonably good fit using this form for both models with  $u_{pk}^{point}(\infty) \approx 1.47 \pm 0.05$  and  $u_{pk}^{fractal}(\infty) \approx 1.00 \pm 0.07$ . Thus, in the case of point-islands, the asymptotic scaled ISD  $f(u)$  appears to diverge at  $u=3/2$  in good agreement with the MF theory prediction [13], while for fractal islands the asymptotic peak position corresponds to  $u_{pk} \approx 1$ .

We now consider the scaled capture-number distribution  $C(s/S) = \sigma_s/\sigma_{av}$ . As can be seen in Fig. 8, for the case of point-islands, the scaled CND is approximately constant, i.e.,  $\sigma_s/\sigma_{av} = 1$ , for  $s/S < 3/2$ . This is in good agreement with the MF theory prediction, as well as with previous point-island model simulations in 3D [26]. In this case, the crossing of the scaled CND and the line  $zu$  (with  $z=3/2$ ) near  $u=3/2$  indicates a divergence in the scaled ISD in good agreement with the ISD results shown earlier. In contrast, for the fractal model with  $z=1$ , we find that for large enough coverage ( $\theta = 0.06$ ), the scaled CND increases approximately linearly with scaled island size, i.e.,  $C(u) \approx zu$  (see Fig. 8) [31]. This result is quite surprising since it implies that both the numerator and denominator in Eq. (4) approach zero in the asymptotic limit. Since Eq. (4) implies that any possible divergence in the scaled ISD is due to a divergence in the ratio  $[2z-1-C'(u)]/[C(u)-zu]$ , the fact that *both* the numerator and denominator approach zero may explain the relatively weak apparent divergence of the ISD in this case. We note that the linear dependence of the capture number on island size cannot be explained by the explicit dependence on island size  $s$  exhibited by Eq. (9), i.e.,  $\sigma_s = 4\pi r_s(1+r_s/\xi)$ . Accordingly, we expect that correlations between the size of an island and its capture zone, which are not included in the self-consistent RE theory, play an important role for the case of fractal islands in  $d=3$ .

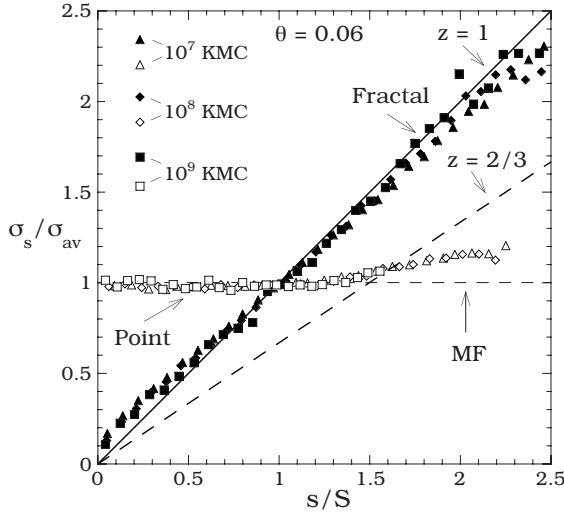


FIG. 8. Scaled CND for  $D_h/F=10^7$  (triangles),  $10^8$  (diamonds), and  $10^9$  (squares) for point-islands (open symbols) and fractal islands (closed symbols). Also indicated are the lines  $zu$  with  $z=2/3$  for point-islands and  $z=1$  for fractal islands, as well as the MF prediction  $C(u)=1$ .

#### IV. DISCUSSION

Motivated by previous work [26] on the irreversible nucleation and growth of point-islands in  $d=3$  in which MF-like behavior, corresponding to  $C(u)=1$  and a scaled ISD which diverges with increasing  $D/F$ , were observed, we have carried out simulations and RE calculations for the irreversible nucleation and growth of fractal islands in  $d=3$ . In contrast to the results previously obtained for point-islands, we find that for fractal islands the scaled CND deviates *strongly* from MF behavior and, in particular, is approximately linear in the asymptotic limit. In addition, while the scaled ISD appears to diverge with increasing  $D/F$ , the divergence is much weaker than in the case of point-islands. We also note that for fractal islands, the peak of the ISD occurs near  $s/S=1$ , which is quite different from the value ( $u=3/2$ ) obtained for point-islands. Thus, our results indicate that in  $d=3$ , the island fractal dimension  $d_f$  plays a strong role in determining the asymptotic scaled ISD and CND. We note that this is in contrast to previous results in  $d=1$  [19] and  $d=2$  [13,18], in which significant deviations from MF behavior were found for both point-islands and fractal (extended) islands.

For comparison with these results, we have also carried out simulations of a point-island model in  $d=3$  which is somewhat different from the point-island model studied in Ref. [26], and for which the short-range interaction is similar to that in our fractal-island model. In good agreement with the previous results obtained for a point-island model with a shorter range of interaction (SSA model) in Ref. [26], we find that for point-islands in  $d=3$ , the scaled ISD diverges with increasing  $D/F$  while the corresponding asymptotic scaled CND is very close to the MF prediction  $C(u)=1$ . However, we note that the ISD diverges less rapidly than predicted by pure MF behavior [see Fig. 4(a)], while the value of the exponent  $\phi$  describing the dependence of the

ISD peak height on  $D/F$  ( $\phi \approx 0.06$ ) is slightly smaller than the MF RE value  $\phi_{MF} \approx 0.08$ .

We have also compared our simulation results for the average island and monomer densities with the results of a self-consistent RE calculation and good agreement was obtained for both point and fractal islands. In particular, we determined the exponent  $\chi$ , which describes the dependence of the island density at fixed coverage in the aggregation regime (e.g., the “saturation” island density) on  $D/F$ . For the case of point-islands (corresponding to island fractal dimension  $d_f=\infty$ ), we found  $\chi \approx 1/3$  in good agreement with the MF RE prediction. However, for fractal islands a significantly larger value ( $\chi \approx 0.42$ ) was obtained in both our simulations and RE calculations.

In order to understand the large value obtained for fractal islands, we have also derived an analytic expression for  $\chi$  as a function of island fractal dimension  $d_f$  in  $d=3$ . In particular, based on the assumption that the majority of island nucleation occurs when  $r_s/\xi \lesssim 1$ , we find  $\chi = d_f / (3d_f - 2)$  in the limit of large  $D/F$ . For the case of fractal islands with  $d_f=2.5$ , this leads to  $\chi \approx 0.45$ , which is in reasonable agreement with the value obtained in our simulations ( $\chi \approx 0.42$ ). We also note that for compact islands with  $d_f=3$ , this leads to  $\chi = 3/7 \approx 0.43$  in good agreement with the corresponding self-consistent RE calculation results. In addition, we note that for point-islands with  $d_f=\infty$ , this expression leads to  $\chi = 1/3$  in good agreement with our simulation results as well as with the standard prediction [6] for irreversible growth.

Interestingly, if instead of assuming that the majority of island nucleation occurs when  $r_s/\xi \lesssim 1$ , we instead assume that the majority of island nucleation occurs when  $r_s/\xi \gg 1$ , then combining Eq. (12b) with Eq. (16) leads to a somewhat different expression for  $\chi$ , i.e.,  $\chi = d_f / (5d_f - 8)$ . Since  $r_s/\xi$  exhibits no  $D/F$  dependence for  $d_f=3$  [see Eq. (11)], for compact islands this leads to the same value for  $\chi$  as given by Eq. (17). In contrast, for fractal islands with  $d_f \approx 2.5$ , it leads to a significantly higher value, e.g.,  $\chi \approx 0.55$ . However, this result contradicts the known [9] scaling of the crossover coverage  $\theta_x \sim R^{-1/2}$  (where  $\theta_x$  corresponds to the coverage at which the island density  $N$  equals the monomer density  $N_1$ ), thus, confirming our assumption that in general  $r_s/\xi < 1$  in the nucleation regime.

As a further test of this assumption, we have also used our REs to calculate  $r_s/\xi$  for the case of fractal islands with  $D_h/F=10^7-10^9$  at a coverage  $\theta=0.01$  when most of the islands have already nucleated [see Fig. 2(a)]. As expected, while  $r_s/\xi$  increases with coverage, we find  $r_s/\xi < 1$  for  $D_h/F=10^7-10^9$  and  $\theta=0.01$ . In addition, numerical RE results for the scaling behavior of  $r_s/\xi$  and  $\sigma_{av}$  at  $\theta=0.01$  for fractal islands with  $d_f \approx 2.5$  (e.g.,  $r_s/\xi \sim R^x$  and  $\sigma_{av} \sim R^y$  with  $x \approx 0.050$  and  $y \approx 0.18$ ) are in good agreement with the values  $\{x=3d_f/[2(3d_f-2)] \approx 0.045, y=1/(3d_f-2) \approx 0.18\}$  predicted using Eqs. (11a) and (12a) based on the assumption that  $r_s/\xi < 1$ .

Since the general problem of the dependence of the island density on  $D/F$  may be of some interest, we note that the arguments used to obtain Eq. (17) may be generalized to obtain an expression for the exponent  $\chi$  as a function of the critical island size  $i$ , island fractal dimension  $d_f$ , and exponent  $\eta$ , describing the dependence of the capture number  $\sigma_s$

on island radius  $r_s$  (e.g.,  $\sigma_s \sim r_s^\eta$ ) in the nucleation regime  $r_s/\xi < 1$ , which is valid for  $d \geq 2$ . In particular, assuming the Walton relation [3]  $N_i \sim N_1^i$ , replacing  $N_1^2$  in Eq. (15) by  $N_1^{i+1}$  and modifying Eqs. (14)–(16) accordingly, leads to the general result,

$$\chi = \frac{id_f}{(i+2)d_f - (i+1)\eta}. \quad (18)$$

In general, we expect  $\eta = d - 2$ . For the case of point-islands with  $d_f = \infty$ , as well as for the case of  $d = 2$  (for which  $\eta = 0$  with logarithmic corrections [11]), this implies  $\chi = i/(i+2)$  in agreement with the standard expression [6] for submonolayer island growth with a critical island size equal to  $i$ . However, for  $d > 2$  and finite  $d_f$ , Eq. (18) implies significant deviations from the standard expression, as well as a significant dependence on  $d_f$ . In particular, assuming  $i = 1$  and  $\eta = 1$  (corresponding to  $d = 3$ ), leads again to Eq. (17). It is also interesting to compare this result with that obtained in Ref. [32] for the case of submonolayer island growth in  $d = 2$ , e.g.,  $\chi = 2i/(2i + 2 + d_f)$ . While this expression is reasonably accurate for compact and fractal islands in  $d = 2$ , for point-islands, it implies  $\chi = 0$  which is incorrect. Thus, a correct analysis of the dependence of the scaling exponent  $\chi$  on island fractal dimension  $d_f$  is not as simple as had been assumed.

We now return to the shape of the scaled CND for the case of fractal islands. As already noted, the approximate linear dependence of  $\sigma_s$  on island size  $s$  obtained in this case cannot be explained simply by the capture-number expression, Eq. (9), since this predicts at most an  $s^{2/2.5}$  dependence. Thus, in contrast to the behavior for point-islands in  $d = 3$  (for which the MF behavior of the CND indicates the complete absence of correlation between the size of an island and its capture zone), our results indicate that for fractal islands in  $d = 3$ , there is a significant correlation between the island size  $s$  and the local capture length (or capture zone)  $\xi_s$ . We also note that the apparent crossing of  $C(u)$  and  $zu$  at  $u = 1$ , would seem to indicate a divergence of the ISD with increasing  $D/F$  as suggested by Eq. (4). However, it also appears that with increasing  $D/F$  the scaled CND is approaching the asymptotic form  $C(u) = zu$ . This leads to an indeterminate form for the argument of the exponential in Eq. (4) since the numerator and denominator in the ratio  $[2z - 1 - C'(u)]/[C(u) - zu]$  both approach zero, and thus may explain the relatively weak apparent divergence of the ISD in this case. In this connection, it is worth noting that as pointed out in Ref. [33], for  $z = 1$  and  $C(u) = u$ , the asymptotic ISD is not uniquely determined by the asymptotic CND but rather depends on the nucleation history in the early-coverage regime. This case has also been discussed in Ref. [21] in the context of approximate scaling forms for nucleation capture zones and capture zone area distributions.

In order to determine if the same behavior occurs for the case of fractal islands in 2D, we have measured the scaled CND for this case at a coverage ( $\theta = 0.3$ ) near the end of the precoalescence regime. As can be seen in Fig. 9, in this case

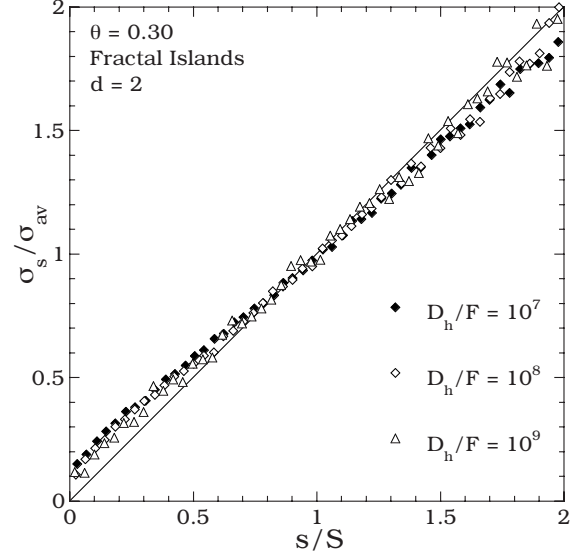


FIG. 9. Scaled CND as a function of  $R_h$  for fractal islands in  $d = 2$ .

the scaled CND also crosses the line  $zu$  but also appears to be approaching linear behavior in the asymptotic limit. As shown by the dashed line in Fig. 6, in  $d = 2$  the ISD also appears to be diverging with increasing  $D/F$ , although somewhat more weakly than in 3D. Thus, it would appear that while there are clearly significant differences for point-islands in the behavior of the ISD and CND in  $d = 2$  and  $d = 3$ , for fractal islands the behavior is rather similar.

Finally, we note that the results presented here for irreversible nucleation and growth in  $d = 3$  correspond to two extreme limits: the point-island limit (corresponding to complete “rearrangement” of islands and  $d_f = \infty$ ) and the fractal-island limit (corresponding to the complete absence of rearrangement and  $d_f \approx 2.5$ ). As our results indicate, while the scaled ISD appears to diverge with increasing  $D/F$  in both cases, the divergence is much weaker for fractal islands than for point-islands. Similarly, the scaled CND for fractal islands is completely different from that for point-islands. Given these differences (as well as the fact that cluster rearrangement is generally to be expected), it would be of interest to carry out simulations for the case of compact islands with  $d_f = 3$ . In particular, it would be interesting to find out if the dependence of the ISD on  $D/F$  for compact islands is closer to that for point-islands or fractal islands. We are currently carrying out simulations for this case in order to determine if the existence of island relaxation leads to significant differences from the results presented here.

#### ACKNOWLEDGMENTS

This work was supported by the NSF through Grants No. DMR-0606307 and No. CCF-0840389. We would also like to acknowledge grants of computer time from the Ohio Supercomputer Center (Grant No. PJS0245).

- [1] J. W. Evans, P. A. Thiel, and M. C. Bartelt, *Surf. Sci. Rep.* **61**, 1 (2006).
- [2] Z. Y. Zhang and M. G. Lagally, *Science* **276**, 377 (1997).
- [3] D. Walton, *J. Chem. Phys.* **37**, 2182 (1962); D. Walton, T. N. Rhodin, and R. W. Rollins, *ibid.* **38**, 2698 (1963).
- [4] J. A. Venables, G. D. Spiller, and M. Hanbucken, *Rep. Prog. Phys.* **47**, 399 (1984).
- [5] R. Kunkel, B. Poelsema, L. K. Verheij, and G. Comsa, *Phys. Rev. Lett.* **65**, 733 (1990).
- [6] J. A. Venables, *Philos. Mag.* **27**, 697 (1973).
- [7] M. C. Bartelt and J. W. Evans, *Phys. Rev. B* **46**, 12675 (1992).
- [8] J. W. Evans and M. C. Bartelt, *J. Vac. Sci. Technol. A* **12**, 1800 (1994).
- [9] J. G. Amar, F. Family, and P. M. Lam, *Phys. Rev. B* **50**, 8781 (1994).
- [10] C. Ratsch, A. Zangwill, P. Smilauer, and D. D. Vvedensky, *Phys. Rev. Lett.* **72**, 3194 (1994).
- [11] G. S. Bales and D. C. Chrzan, *Phys. Rev. B* **50**, 6057 (1994).
- [12] J. G. Amar and F. Family, *Phys. Rev. Lett.* **74**, 2066 (1995).
- [13] M. C. Bartelt and J. W. Evans, *Phys. Rev. B* **54**, R17359 (1996).
- [14] J. A. Blackman and P. A. Mulheran, *Phys. Rev. B* **54**, 11681 (1996).
- [15] P. A. Mulheran and J. A. Blackman, *Surf. Sci.* **376**, 403 (1997).
- [16] P. A. Mulheran and D. A. Robbie, *Europhys. Lett.* **49**, 617 (2000).
- [17] J. G. Amar, M. N. Popescu, and F. Family, *Phys. Rev. Lett.* **86**, 3092 (2001).
- [18] M. N. Popescu, J. G. Amar, and F. Family, *Phys. Rev. B* **64**, 205404 (2001).
- [19] J. G. Amar, M. N. Popescu, and F. Family, *Surf. Sci.* **491**, 239 (2001).
- [20] J. W. Evans and M. C. Bartelt, *Phys. Rev. B* **63**, 235408 (2001).
- [21] J. W. Evans and M. C. Bartelt, *Phys. Rev. B* **66**, 235410 (2002).
- [22] J. A. Venables and H. Brune, *Phys. Rev. B* **66**, 195404 (2002).
- [23] J. G. Amar and M. N. Popescu, *Phys. Rev. B* **69**, 033401 (2004).
- [24] P. A. Mulheran, *Europhys. Lett.* **65**, 379 (2004).
- [25] M. von Smoluchowski, *Z. Phys. Chem.* **17**, 557 (1916); **92**, 129 (1917).
- [26] F. Shi, Y. Shim, and J. G. Amar, *Phys. Rev. B* **71**, 245411 (2005).
- [27] F. Shi, Y. Shim, and J. G. Amar, *Phys. Rev. E* **74**, 021606 (2006).
- [28] F. Shi, Y. Shim, and J. G. Amar, *Phys. Rev. E* **79**, 011602 (2009).
- [29] T. A. Witten, Jr., and L. M. Sander, *Phys. Rev. Lett.* **47**, 1400 (1981).
- [30] P. Meakin, *Phys. Rev. A* **27**, 1495 (1983).
- [31] We note that the agreement between our KMC results for the scaled CND for fractal islands at  $\theta=0.06$  and the expression  $C(u)=u$  tends to improve with increasing  $D/F$ . However, at slightly lower coverages, the scaled CND deviates more significantly from this expression.
- [32] M. Schroeder and D. E. Wolf, *Phys. Rev. Lett.* **74**, 2062 (1995).
- [33] D. D. Vvedensky, *Phys. Rev. B* **62**, 15435 (2000).